1　Field-Based High-Throughput Plant Phenotyping Reveals the Temporal Patterns of Quantitative

2　Trait Loci Associated with Stress-Responsive Traits in Cotton

3

4　Duke Pauli[*], Pedro Andrade-Sanchez[†], A. Elizabete Carmo-Silva[‡,1], Elodie Gazave[*], Andrew N.

5　French[‡], John Heun[†], Douglas J. Hunsaker[‡], Alexander E. Lipka[§], Tim L. Setter[††], Robert J.

6　Strand[‡,2], Kelly R. Thorp[‡], Sam Wang[‡‡,3], Jeffrey W. White[‡] and Michael A. Gore[*,4]

7

8　[*]Plant Breeding and Genetics Section, School of Integrative Plant Science, Cornell University,

9　Ithaca, NY 14853, USA

10　[†]Department of Agricultural and Biosystems Engineering, University of Arizona, Maricopa

11　Agricultural Center, Maricopa, AZ 85138, USA

12　[‡]United States Department of Agriculture–Agricultural Research Service (USDA-ARS), Arid-

13　Land Agricultural Research Center, Maricopa, AZ 85138, USA

14　[§]Department of Crop Sciences, University of Illinois, Urbana, IL 61801, USA

15　[††]Soil and Crop Sciences Section, School of Integrative Plant Science, Cornell University, Ithaca,

16　NY 14853, USA

17　[‡‡]School of Plant Sciences, University of Arizona, Maricopa Agricultural Center, Maricopa, AZ

18　85138, USA

19

20　[1]Present address: Lancaster Environment Centre (LEC), Lancaster University, LA1 4YQ, UK

21　[2]Present address: LemnaTec Corporation, Saint Louis, MO 63110

22　[3]Present address: Bridgestone Americas, Inc., Eloy, AZ 85131

23　[4]Corresponding author

24   Running Title: High-Throughput Phenotyping of Cotton

25

26   Keywords:

27   Field-based HTPP

28   Stress response

29   Canopy temperature

30   NDVI

31   QTL

32

33   Corresponding author:

34   Michael A. Gore

35   310 Bradfield Hall

36   Cornell University

37   Ithaca, NY 14853

38   Email: mag87@cornell.edu

39   Phone: 607-255-5492

40

ABSTRACT

41

42   The application of high-throughput plant phenotyping (HTPP) to continuously study plant

43   populations under relevant growing conditions creates the possibility to more efficiently dissect

44   the genetic basis of dynamic adaptive traits. Towards this end, we employed a field-based HTPP

45   system that deployed sets of sensors to simultaneously measure canopy temperature, reflectance,

46   and height on a cotton (*Gossypium hirsutum* L.) recombinant inbred line mapping population.

47   The evaluation trials were conducted under well-watered and water-limited conditions in a

48   replicated field experiment at a hot, arid location in central Arizona, with trait measurements

49   taken at different times on multiple days across three years. Canopy temperature, normalized

50   difference vegetation index (NDVI), height, and leaf area index (LAI) displayed moderate to

51   high broad-sense heritabilities as well as varied interactions among genotypes with water regime

52   and time of day. Distinct temporal patterns of quantitative trait loci (QTL) expression were

53   mostly observed for the more dynamic HTPP canopy traits, canopy temperature and NDVI, and

54   varied across plant developmental stages. In addition, the strength of correlation between HTPP

55   canopy and agronomic traits such as lint yield displayed a time-dependent relationship. We also

56   found that the position of some QTL controlling HTPP canopy traits were shared with agronomic

57   and physiological traits. This work demonstrates the novel use of a field-based, HTPP system to

58   study the genetic basis of stress-adaptive traits in cotton, and these results have the potential to

59   facilitate the development of stress-resilient cotton cultivars.

60

INTRODUCTION

Cotton (*Gossypium* spp.) is the top renewable textile fiber in the world, supporting a multibillion dollar industry with a global production of 26.2 million metric tons in 2014 (Cotton Inc. 2015). The United States is the third largest producer with its 2014 crop valued at over $5 billion, generating $25 billion in products and services (USDA-NASS 2015, USDA-ERS 2015). The future sustainability of US cotton production, however, is threatened by climatic changes because nearly 60% of cotton acreage depends on dryland (rainfed) agricultural production systems (National Cotton Council of America 2015). Due to this reliance on precipitation for crop production, the effects of global climate change, including decreased rainfall, increased temperatures, and highly variable weather patterns, pose an imminent risk to cotton production.

Water deficit and high temperature are significant abiotic stresses which often coincide in the production environment and can dramatically reduce crop yields (Rizhsky et al. 2002). In cotton, impacts of high heat, drought, and their combined effects include reproductive limitations through abnormal floral development and fertilization, reduced photosynthetic capacity, impaired photoassimilate distribution, and generation of reactive oxygen species (Burke and Wanjura 2010; Loka et al. 2011; Dabbert and Gore 2014). These factors negatively impact lint yield through numerous avenues including earlier floral cutout, decreased nodes above white flower, reduction in the number of bolls, and impaired carbon assimilation (Chaves et al. 2003; Pettigrew 2004). To cope with these environmental challenges, cotton employs mechanisms to regulate water usage and maintain thermal stability including the use of evaporative cooling through increased stomatal conductance. To investigate the relationship between stomatal conductance and leaf temperature, Radin et al. (1994) constructed a Pima cotton (*G. barbadense* L.) population in which these two traits were cosegregating and evaluated the population in a

84   hot, arid environment. They observed a strong inverse relationship between leaf temperature and

85   stomatal conductance as well as a significant correlation between cooler canopies and boll set.

86   Such an increase in transpiration rate serves as a mechanism for "heat avoidance," thereby

87   allowing for the maintenance of plant function.

88   The development of cultivars possessing tolerance to heat and drought stress is a major

89   consideration of many cotton breeding programs. However, progress has been hampered by a

90   limited understanding of the key genes and alleles that underlie physiological and developmental

91   mechanisms and how they relate to productivity under abiotic stress, highlighting the current

92   challenge of connecting genotype to phenotype. Despite the substantial evolution of DNA

93   sequencing technologies over the past 10 years, collection of data for important physiological

94   and developmental phenotypes on large populations remains onerous (Furbank and Tester 2011;

95   Davey et al. 2011). In particular, the process of obtaining highly heritable phenotypes associated

96   with tolerance to heat and drought stress is particularly burdensome given that environmental

97   conditions in which phenotypes were collected are nearly impossible to replicate across field

98   locations and years (Campos et al. 2004; Araus and Cairns 2014). The challenges of collecting

99   such data for dynamic traits are further compounded because their observed values are partially

100   dependent upon ambient environmental conditions that could drastically vary within and

101   between days of a single year.

102   The continued technological advancement of field-based high-throughput plant

103   phenotyping (HTPP) tools has been strongly advocated to address the phenotyping needs of the

104   plant science community (White et al. 2012). As one form of proximal sensing, HTPP typically

105   relies on quantifying the interaction of electromagnetic radiation with the plant canopy using

106   various sensors in close proximity to the plants (Mulla 2013). Due to the non-contact nature of

107   the sensors and their placement on vehicles capable of traversing research plots at a rapid pace,

108   HTPP systems are capable of collecting vast amounts of data in an efficient manner (Andrade-

109   Sanchez et al. 2014; White et al. 2012; Busemeyer et al. 2013). The ability to collect data rapidly

110   also permits comprehensive assessment of crop development, and with it, the ability to map QTL

111   expression as a function of time, which is critical given that most traits of agronomic and

112   economic importance are dynamic in nature (Wu and Lin 2006; Würschum et al. 2014). Despite

113   awareness of this reality, the majority of QTL studies rely on phenotypic data collected at a

114   single time point, offering only a final view of accumulated QTL effects. By implementing an

115   HTPP system that is capable of collecting data throughout the season under actual production

116   conditions, it becomes possible for researchers to more fully understand the complexities of trait

117   development and with this to better optimize genotypes through selection in breeding programs.

118   In the present study, we used a high-clearance tractor retrofitted with a suite of sensors to

119   collect data on canopy properties including canopy temperature, reflectance, and height for

120   characterizing a cotton (*G. hirsutum* L.) mapping population of 95 recombinant inbred lines

121   (RILs) under contrasting irrigation regimes. In addition, physiological, agronomic, and fiber

122   quality data were collected so that their genetic relationship with HTPP canopy traits could be

123   investigated. The objectives of this study were to (i) identify QTL responsible for the dynamic

124   response of HTPP canopy traits to the abiotic stresses of high temperature and water deficit, (ii)

125   evaluate the temporal patterns of QTL expression over the reproductive phase of the plant

126   lifecycle, and (iii) examine the genetic relationship of HTPP canopy traits with agronomic,

127   physiological, and fiber quality traits.

128   **MATERIALS AND METHODS**

129   **Plant materials and experimental design**

130   The TM-1×NM24016 mapping population (Gore et al. 2012; Percy et al. 2006) of 95

131   recombinant inbred lines (RILs) was evaluated at the Maricopa Agricultural Center (MAC) of

132   the University of Arizona located in Maricopa, AZ (33°04'37" N, 111°58'26" W, elevation 358

133   m) in three consecutive years (2010-12). The set of repeated parental lines (TM-1 and

134   NM24016), repeated commercial check cultivars (DP 491, FM 958, STV 457, STV 506, and DP

135   393), and the 95 RILs, was evaluated under well-watered (WW) and water-limited (WL)

136   conditions. The experimental field trials were planted on days 127, 117, and 117 (Julian

137   calendar) in 2010, 2011, and 2012, respectively. In each year, the experimental trial was

138   arranged as an 11 x 10 α (0, 1) lattice design with two replications, with a total of 440 plots. The

139   order of entries within each incomplete block was randomized. In addition, the positions of

140   replicates within the experimental field were randomized across years. To reduce edge effects, a

141   conventional commercial upland cotton cultivar was planted on all sides of each replicate.

142   Experimental units were one-row plots 8.8 m in length with a 0.61 m alley at the end of each

143   plot. Plots were thinned to a density of ~4.1 plants m^{-2} and had an inter-row spacing of 1.02 m.

144   The soil type is a Casa Grande sandy loam (fine-loamy, mixed, superactive, hyperthermic Typic

145   Natrargids). Conventional cotton cultivation practices for the desert Southwest were employed.

146   Meteorological data were obtained from an automated Arizona Meteorological Network

147   (AZMET) weather station (ag.arizona.edu/azmet/index.html) located 270 m from the field

148   (Brown 1989).

149   Several furrow irrigations were applied during the first 10-14 days after planting to

150   establish the crop after which subsurface drip irrigation (SDI) was used for the remainder of the

151   field season. The scheduling of SDI was performed using a daily soil water balance model

152   calculated for the cotton root zone as previously described in Andrade-Sanchez et al. (2014). Soil

7

153   water balance model inputs included estimated daily evapotranspiration as determined from

154   FAO-56 crop coefficient procedures (Allen et al. 1998), metered irrigation depths, and

155   precipitation data from the AZMET weather station. Soil water characteristics used in the soil

156   water balance were as those presented in Hunsaker et al. (2005; table 3) for the sandy loam soil.

157   Irrigations to the WW plots were applied to refill the root zone water content to field capacity at

158   approximately 35% soil water depletion. Starting mid-July, the WL plots received one half of the

159   irrigation amounts applied to the WW plots. The WL treatment was imposed when more than

160   50% of the plots were at first flower to minimize the interaction of phenology and soil moisture

161   deficit. Weekly soil water content measurements in 0.2 m increments from a depth of 0.1 to 1.5

162   m were made in plots to monitor the actual soil water depletion and adjust the modeled soil water

163   balance when needed.

164   **Phenotyping of agronomic, fiber, and physiological traits**

165   The RIL population, parental lines, and commercial check cultivars were phenotyped for a

166   number of agronomic, fiber quality, and physiological traits. The classification of the RIL

167   population for distinct cotton plant developmental stages (flowering/peak bloom; boll

168   development and fill; fiber development and elongation) was based on the number of days after

169   planting and within field plant phenological observations following Oosterhuis (1990).

170   Throughout the growing season and after mechanical harvest, median plant height for each plot

171   was manually measured with a calibrated bar-coded ruler according to Andrade-Sanchez et al.

172   (2014). At the end of the season, plots were mechanically harvested using a one-row harvester.

173   Prior to this, 25 bolls were harvested by hand from each plot and processed using a laboratory

174   10-saw gin to collect boll and fiber data. The following phenotypic data were gathered on the

175   boll and fiber samples: boll size (grams boll^{-1}), lint yield (kg ha^{-1}), and seeds per boll. The fiber

176   quality traits measured were fiber elongation (percent), strength (kN m kg^{-1}), uniformity

177   (percent), micronaire (unit), and length (upper half mean, mm). Fiber quality measurements were

178   made using an Uster HVI 1000 (High Volume Instrument, Uster, Charlotte, NC, US) at Cotton

179   Incorporated (Cary, NC, US).

180   The concentrations of abscisic acid (ABA, picomolar per cm^2) and soluble sugar (sucrose

181   and glucose, micromolar per cm^2) were quantified in leaf tissue using an enzyme-linked

182   immunosorbant assay (ELISA) following the method of Setter et al. (2010) with additional

183   information provided in Setter et al. (2001). Briefly, in 2011 and 2012, leaf tissue samples were

184   taken from six representative plants of each plot with one leaf disc sample taken per plant. Each

185   leaf disc was collected from the upper lobe of a fully expanded leaf near the third node of the

186   plant. Leaf disc samples were collected on days 237 and 242 (Julian calendar) in 2011 and 2012,

187   respectively, which corresponded to the fiber development and elongation phase of cotton plant

188   development. Leaf discs were taken with a 6 mm punch and sampled directly into 1.2 mL tubes

189   of a 96-well plate that was promptly stored on ice in a Styrofoam cooler until brought out of the

190   field. Once transferred to the lab, tissue samples were then properly preserved until measuring

191   their concentration of ABA and soluble sugar.

192   Carbon isotope composition analysis was performed on leaf tissue samples by the

193   University of California, Davis Stable Isotope Facility (Davis, CA, US). In 2010-12, leaf disc

194   samples were collected in the same manner as performed for the quantification of ABA and

195   soluble sugar. In 2010, leaf disc samples were collected on day 231 (Julian calendar), which

196   corresponded with the end of cotton boll development and fill. In 2011 and 2012, leaf disc

197   samples were collected on days 251 and 249 (Julian calendar), respectively, which coincided

198   with cotton fiber development and elongation. Dried leaf tissue samples were ground to a fine

199 powder, followed by the weighing and placing of 1-2 mg subsamples into capsules. Carbon

200 isotope composition was determined with an isotope ratio mass spectrometer (Sercon Ltd.,

201 Cheshire, UK), and calculated as $\delta^{13}C$ (‰) relative to the international Vienna Pee Dee

202 Belemnite (V-PDB) reference standard (Farquhar et al. (1989). Carbon isotope discrimination

203 ($\Delta^{13}C$) was then estimated by the method of Farquhar et al. (1989).

204 **HTPP of canopy traits**

205 We employed an HTPP system to rapidly collect proximally sensed plant canopy temperature,

206 reflectance, and height data from the field experiment over the growing season in 2010-12. The

207 design, development, operational parameters, and field evaluation of this system has been

208 previously described in Andrade-Sanchez et al. (2014). Briefly, a LeeAgra 3434 DL open rider

209 sprayer (LeeAgra, Lubbock, TX, US) was retrofitted with four sets of three sensor types to

210 simultaneously collect phenotypic data from four adjacent rows of experimental plots (i.e., one

211 set of sensors per row). The three types of sensors used were an Apogee SI-121 infrared

212 radiometer (IRT, Apogee Instruments, Logan, UT, US) to measure canopy temperature (°C), a

213 CropCircle ACS-470 multi-spectral crop canopy sensor (Holland Scientific, Lincoln, NE, US) to

214 measure canopy reflectance (ρ) in three 10 nm wavebands with band centers at 670, 720, and 820

215 nm, and a short-range Pulsar dB3 transducer (Pulsar Process Measurement Ltd., Malvern, UK) to

216 measure canopy height (mm). The wavelength data collected from the CropCircle multi-spectral

217 sensors were used to calculate normalized difference vegetation index (NDVI) as follows:

218 $$NDVI = (\rho_{NIR} - \rho_{red}) / (\rho_{NIR} + \rho_{red}), \tag{1}$$

219 where ρ_{NIR} is the spectral reflectance at wavelength 820 nm in the near-infrared waveband region

220 and ρ_{red} is the spectral reflectance at wavelength 670 nm in the red waveband region.

221   To position the HTPP system with centimeter level accuracy, we used a global navigation

222   satellite system (GNSS) real-time kinematics (RTK) global positioning system (GPS) receiver

223   (A320 Smart Antenna, Hemisphere GPS, Scottsdale, AZ, US), a rover receiver mounted at the

224   center of the tractor front-mounted frame, and a separate base station unit (A321 Smart Antenna,

225   Hemisphere GPS) to broadcast high-precision positioning information. Raw data generated by

226   the sensors were stored on three data loggers: CR3000 (Campbell Scientific, Logan, UT, US) for

227   IRT sensors; GeoScout GLS-420 (Holland Scientific, Lincoln, NE, US) for CropCircle multi-

228   spectral sensors; and CR1000 (Campbell Scientific, Logan, UT, US) for ultrasonic proximity

229   sensors. The serial output from the GPS receiver was split in order to send identical positioning

230   data to all three data loggers. The semi-automated geospatial postprocessing of the collected data

231   was performed with custom scripts implemented in the open-source Quantum Geographic

232   Information System software (www.qgis.org) as described in Andrade-Sanchez et al. (2014).

233   In 2010, plant canopy trait data were collected on four different days, while in 2011 and

234   2012 data were collected on nine and seven different days, respectively. Within each day, canopy

235   temperature, reflectance, and height data were usually collected at multiple times of day, ranging

236   from one to three times in 2010 and 2011, to as many as four times per day in 2012. Canopy

237   height measurements were not collected with the HTPP system in 2010. Measurements were

238   taken in the early morning (0700 or 0900), midmorning (1000 or 1100), afternoon (1300), and/or

239   late afternoon (1500) with all times reported in Mountain Standard Time (MST). The time of day

240   (0700, 0900, 1000, 1100, 1300, or 1500) that data were collected is referred as time of day

241   (TOD), while the actual time, measured in minutes, that a measurement was taken is referred to

242   as time of measurement (TOM). The HTPP system only required ~0.5 h to traverse the complete

243   set of experimental plots.

Statistical analyses

To assess whether the non-HTPP (i.e., agronomic, fiber quality, and physiological traits) and postprocessed HTPP (i.e., plant canopy temperature, NDVI, and height traits) data contained significant outliers, we initially fitted a mixed linear model for each trait with the MIXED procedure in SAS for Windows version 9.4 (SAS Institute, Cary, NC). When conducting this analysis, an environment was considered as a separate year for non-HTPP traits and a single day for HTPP traits. For each environment, the fitted model for an individual trait included the main effects of genotype (RILs, parental lines, and commercial check cultivars) and irrigation regime with their two-way interaction as fixed effects; replication nested within irrigation regime and block nested within the two-way interaction of replication and irrigation regime were included as random effects. Degrees of freedom were calculated via the Satterthwaite approximation. The Studentized deleted residuals (Neter et al. 1996) obtained from these mixed linear models were examined to detect outliers. Once significant outliers were removed from the data sets, plot-level averages were calculated with the MEANS procedure in SAS for Windows version 9.4 (SAS Institute).

With the 2011 and 2012 plot-level averages for canopy NDVI and height traits collected by the HTPP system, the method of Scotford and Miller (2004) was used to calculate a compound canopy index (CCI) from which leaf area index (LAI) was estimated as follows:

$$\text{LAI} = \beta \times \text{CCI} = \beta \times (c/c_{max}) \times (h/h_{max}), \tag{2}$$

where β is a constant, c and h are the plot-level averages of canopy cover and height, respectively, for each plot, and c_{max} and h_{max} are respectively the maximum values of canopy cover and height obtained over the growing season. As previously determined from an analysis of height data collected from upland cotton field experiments conducted at MAC from 2009-13,

267   a value of 5.5 was used for β (Thorp et al. 2015).The plot-level averages of NDVI were used as

268   estimates of c.

269   For each non-HTPP trait, an iterative mixed linear model fitting procedure was conducted

270   across years in ASReml-R version 3.0 (Gilmour et al. 2009):

271            $\mathrm{Y}_{ijklmn} = \mu + \mathrm{year}_i + \mathrm{irg}_j + \mathrm{rep(irg} \times \mathrm{year)}_{ijk}$

272            $+ \mathrm{column(rep} \times \mathrm{irg} \times \mathrm{year)}_{ijkl} + \mathrm{block(rep} \times \mathrm{irg} \times \mathrm{year)}_{ijkm}$ (3)

273            $+ \mathrm{genotype}_n + \mathrm{(genotype} \times \mathrm{year)}_{in} + \mathrm{(genotype} \times \mathrm{irg)}_{jn}$

274            $+ \varepsilon_{ijklmn}$,

275   in which Y_{ijklmn} is an individual phenotypic observation; μ is the grand mean; year_i is the effect of

276   the ith year; irg_j is the effect of the jth irrigation regime (WW or WL); $\mathrm{rep(irg} \times \mathrm{year)}_{ijk}$ is the

277   effect of the kth replication within the jth irrigation regime within the ith year; $\mathrm{column(rep} \times \mathrm{irg}$

278    $\times \mathrm{year)}_{ijkl}$ is the effect of the lth plot grid column within the kth replication within the jth

279   irrigation regime within the ith year; $\mathrm{block(rep} \times \mathrm{irg} \times \mathrm{year)}_{ijkm}$ is the effect of the mth incomplete

280   block within the kth replication within the jth irrigation regime within the ith year; $\mathrm{genotype}_n$ is

281   the effect of the nth genotype; $\mathrm{(genotype} \times \mathrm{year)}_{in}$ is the interaction effect between the nth

282   genotype and the ith year; $\mathrm{(genotype} \times \mathrm{irg)}_{jn}$ is the interaction effect between the nth genotype

283   and the jth irrigation regime; and ε_{ijklmn} is the random error term following a normal distribution

284   with mean 0 and variance σ^2. The model terms $\mathrm{genotype}_n$, irg_j, and $\mathrm{(genotype} \times \mathrm{irg)}_{jn}$ were fitted

285   as fixed effects, while all the other terms were fitted as random effects. Likelihood ratio tests

286   were conducted to remove all terms fitted as random effects from the model that were not

287   significant at $\alpha = 0.05$ (Littell et al. 2006).

288   For each of the four HTPP canopy traits (temperature, height, NDVI, and LAI), an

289   iterative repeated measures mixed linear model fitting procedure was conducted separately for

290   each day in ASReml-R version 3.0 (Gilmour et al. 2009):

291     $$Y_{ijklmo} = \mu + tod_i + irg_j + (tod \times irg)_{ij}$$

292     $$+ rep(irg \times tod)_{ijk} + column(rep \times irg \times tod)_{ijkl}$$

293     $$+ block(rep \times irg \times tod)_{ijkm}$$

294     $$+ tom(irg \times tod)_{ijn}$$

295     $$+ genotype_o + (genotype \times tod)_{io} + (genotype \times irg)_{jo} \qquad (4)$$

296     $$+ (genotype \times irg \times tod)_{ijo}$$

297     $$+ \varepsilon_{ijklmno} ,$$

298   with $\varepsilon_{ijklmno}$ equal to $Var(\varepsilon_{ijklmno}) = \sigma^2$, $Cov(\varepsilon_{ijklmno}, \varepsilon_{i'jklmno}) = \rho \sigma^2$, $i \neq i'$

299   in which Y_{ijklmo} is an individual plot-level average; μ is the grand mean; tod_i is the effect of the

300   ith time of measurement within a day; irg_j is the effect of the jth irrigation regime; $(tod \times trt)_{ij}$ is

301   the effect of the interaction between the ith time of measurement within a day and the jth

302   irrigation regime; $rep(irg \times tod)_{ijk}$ is the effect of the kth replication within the jth irrigation

303   regime within the ith time of measurement within a day; $column(rep \times irg \times tod)_{ijkl}$ is the effect

304   of the lth plot grid column within the kth replication within the jth irrigation regime within the ith

305   time of measurement within a day; $block(rep \times irg \times tod)_{ijkm}$ is the effect of the mth incomplete

306   block within the kth replication within the jth irrigation regime within the ith time of

307   measurement within a day; $tom(irg \times tod)_{ijn}$ is the effect of the nth minute the measurement was

308   taken within the jth irrigation treatment within the ith time of measurement within a day;

309     $genotype_o$ is the effect of the oth genotype; $(genotype \times tod)_{io}$ is the effect of the interaction

310   between the oth genotype and the ith time of measurement within a day; $(genotype \times irg)_{jo}$ is the

311 effect of the interaction between the oth genotype and the jth irrigation regime; (genotype $\times$ irg $\times$

312 tod)$_{ijo}$ is the effect of the interaction between the oth genotype, the jth irrigation regime, and the

313 ith time of measurement within a day; and $\varepsilon_{ijklmno}$ is the random error term following a normal

314 distribution with mean 0 and variance σ^2. The residual variance, $\varepsilon_{ijklmno}$, was modeled using a

315 correlated error variance structure that incorporated a constant, non-zero, correlation term (ρ)

316 among error terms to account for correlation among multiple measures on the same experimental

317 unit. The following terms were fitted as fixed effects in the model: tod$_i$; genotype$_o$; irg$_j$;

318 (genotype $\times$ irg)$_{jo}$; (genotype $\times$ tod)$_{io}$; (tod $\times$ irg)$_{ij}$; and (genotype $\times$ irg $\times$ tod)$_{ijo}$. All of the other

319 terms were fitted as random effects. Likelihood ratio tests were conducted to remove all terms

320 fitted as random effects from the model that were not significant at $\alpha = 0.05$ (Littell et al. 2006).

321 The next step of the analysis for each of the non-HTPP and HTPP traits was to detect any

322 remaining influential outliers from the final fitted model on the basis of the DFFITS criterion

323 (Belsley et al. 2004; Neter et al. 1996) in ASReml-R version 3.0 (Gilmour et al. 2009). Once

324 influential observations were removed, the final model (3 or 4) for each trait was refitted to

325 estimate a best linear unbiased estimator (BLUE) for each genotype across years (non-HTPP

326 traits) or within a day (HTPP traits) for the separate irrigation regimes. Sequential tests of fixed

327 effects were conducted with degrees of freedom being calculated with the Kenward and Rogers

328 approximation (Kenward and Roger 1997) in ASReml-R version 3.0 (Gilmour et al. 2009).

329 For each trait, broad-sense heritability on an entry-mean basis ($\hat{H}^2$) was estimated for the

330 separate irrigation regimes using a mixed linear model. Models (3) and (4) were reformulated to

331 remove the irrigation regime term. Next, all terms were then fitted as random effects in order to

332 obtain variance component estimates. The variance component estimates from each final model

333 for a non-HTPP trait were used to estimate $\hat{H}^2$ (Holland et al. 2003) as follows:

$$\hat{H}^2 = \frac{\widehat{\sigma_g^2}}{\widehat{\sigma_g^2} + \dfrac{\widehat{\sigma_{gy}^2}}{n_y} + \dfrac{\widehat{\sigma_\varepsilon^2}}{n_p}} = \frac{\widehat{\sigma_g^2}}{\widehat{\sigma_p^2}}, \qquad (5)$$

where $\widehat{\sigma_g^2}$ is the estimated genetic variance, $\widehat{\sigma_{gy}^2}$ is the estimated variance associated with genotype-by-year variation, $\widehat{\sigma_\varepsilon^2}$ is the residual error variance, n_y is the harmonic mean of the number of years in which each genotype was observed, and n_p is the harmonic mean of the number of plots in which each genotype was observed. The denominator of equation 5 is equivalent to the phenotypic variance, $\widehat{\sigma_p^2}$. The variance component estimates from each final model for a HTPP trait were used to estimate $\hat{H}^2$ (Holland et al. 2003) as follows:

$$\hat{H}^2 = \frac{\widehat{\sigma_g^2}}{\widehat{\sigma_g^2} + \dfrac{\widehat{\sigma_\varepsilon^2}}{n_p}} = \frac{\widehat{\sigma_g^2}}{\widehat{\sigma_p^2}}, \qquad (6)$$

where all terms are as previously defined.

Within an irrigation regime, the Pearson's correlation coefficient (r) was used to estimate the degree of association between BLUEs for each pair of traits at $\alpha = 0.05$ using the *Hmisc* package implemented in R (R Core Team 2014). To allow for the pairwise comparison of non-HTPP vs. HTPP traits within a year, BLUEs for non-HTPP traits were estimated for each year with a reformulation of model (3) that excluded the year term. The Bonferroni correction was used to control for the multiple testing problem at $\alpha = 0.05/k$, with k equal to the number of comparisons.

QTL analysis

357 The marker genotyping of and genetic linkage map construction for the TM-1×NM24016

358 mapping population have been previously described in Gore et al. (2014). Briefly, the linkage

359 map consisted of 429 simple-sequence repeat (SSR) and 412 genotyping-by-sequencing (GBS)-

360 based single-nucleotide polymorphism (SNP) marker loci, covering about 50% of the tetraploid

361 cotton genome. These 841 marker loci were assigned to 117 linkage groups, with the number of

362 markers included in each linkage group ranging from 2 to 57. The linkage map covered a total of

363 ~2,061 cM of the tetraploid cotton genome, and the 841 loci were not equally distributed across

364 all 26 chromosomes.

365 The BLUEs of each non-HTPP trait were used separately to map additive QTL effects in

366 each irrigation regime with inclusive composite interval mapping (ICIM) (Li et al. 2007) for

367 biparental populations (BIP) in the QTL IciMapping v. 4.0 software

368 (https://www.integratedbreeding.net). The two stages of the ICIM method have been previously

369 described in Gore et al. (2014). In the first stage, the thresholds for individual markers to enter

370 and exit the general linear model via a stepwise regression procedure was set at $P = 1 \times 10^{-4}$ and

371 $P = 2 \times 10^{-4}$, respectively, for an overall Type I error rate of $\alpha = 0.05$ based on a permutation

372 procedure run 1000 times (Anderson and Braak 2003). In the second stage, we conducted a one-

373 dimensional scan across the entire genome at 1-cM steps based on coefficient estimation in the

374 first stage. In order to select the logarithm of the odds (LOD) threshold for an experiment-wise

375 Type I error rate of $\alpha = 0.05$, a permutation procedure was run 1000 times (Churchill and Doerge

376 1994) for each trait in the QTL IciMapping v4.0 software. The LOD thresholds had an average

377 LOD value of 3.3.

378 We used the BLUEs of each HTPP trait to separately map additive QTL effects and their

379 interaction with the environment (QTL-by-environment interaction, QEI) for each irrigation

17

380   regime with ICIM for multi-environment trials (MET) (Li et al. 2015) in the QTL IciMapping v.

381   4.0 software. Each day within a year was analyzed independently with time points within a day

382   each considered an environment. Therefore, QTL were mapped across multiple times within a

383   day for an irrigation regime. The two stages of the ICIM MET method are similar to that of

384   ICIM BIP. In the first stage, a permutation procedure was run 1000 times (Anderson and Braak

385   2003) to set an overall Type I error rate at $\alpha = 0.05$, resulting in an entry threshold of $P = 1 \times 10^{-4}$

386   ^{4} and exit threshold of $P = 2 \times 10^{-4}$ that were used to fit individual markers by stepwise

387   regression in a general linear model. In the second stage, for each trait, a one-dimensional scan

388   was carried out across the entire genome at 1-cM steps at an experiment-wise Type I error rate of

389    $\alpha = 0.05$ (average LOD value of 3.3) as determined by a permutation procedure run 1000 times

390   (Churchill and Doerge 1994) in the QTL IciMapping v4.0 software. The criterion used to declare

391   coincident QTL between traits was based on at least a 10 cM overlap in QTL intervals on the

392   linkage map.

393   To localize markers on the allotetraploid cotton (*G. hirsutum* L. acc. TM-1) draft genome

394   sequence, we downloaded sequence information for the 26 pseudochromosomes (NBI assembly

395   v1.1; http://www.cottongen.org) (Zhang et al. 2015). The BLASTN algorithm in the BLAST+

396   version 2.2.29 package (stand-alone) (Camacho et al. 2009) was used to align context nucleotide

397   sequences of SNP and SSR markers to the reference genome sequence. These BLASTN results

398   were used to tentatively assign the 117 linkage groups to the 26 pseudochromosomes and

399   approximate the physical proximity of mapped markers defining QTL intervals to annotated

400   genes in the TM-1 draft genome sequence. To assign linkage groups, we relied on majority

401   agreement among markers within a linkage group (e.g., if 20 of 25 markers from a linkage group

402   were placed on A01 and the remaining five markers were placed on D01, that linkage group was

403   assigned to A01). For cases when agreement among markers was ambiguous (only occurred for

404   relatively smaller linkage groups), we also considered marker sequence length giving preference

405   to those markers with longer context sequence lengths and higher percent matching to the TM-1

406   draft genome. The values for the percent identity match between marker sequences and the TM-1

407   draft genome ranged from a minimum of 94.4% to a maximum of 99.9% with an average of

408   98.5%. The NBI_Gossypium_hirsutum_v1.1.gene.gff3 annotation file

409   (http://www.cottongen.org) was used to extract candidate gene information.

410   BLUEs from the fitted linear mixed models for both HTPP and non-HTPP traits are

411   contained in File S1. Accompanying genotypic data for the 95 RILs are contained in File S2 with

412   accompany linkage map information. File S3 contains linkage map information for the TM-

413   1×NM24016 RIL population integrated with the published TM-1 draft genome sequence.

414   **RESULTS**

415   **Meteorological conditions at the experimental field site**

416   The summer meteorological conditions of the experimental field site in the low desert of central

417   Arizona served as an optimal environment for assessing the effects of heat and drought stress on

418   the levels of phenotypic variation in the TM-1×NM24016 cotton recombinant inbred mapping

419   population during the 2010-12 field seasons. However, it was not possible to impose drought

420   stress in the absence of high temperature, as this would require a cooler, arid environment such

421   as at a higher elevation in Arizona. The average air temperature during daytime hours (0700-

422   1600 hours MST) was 35° from June (early reproductive) to September (boll and fiber

423   maturation) ― the time period of the growing season in which the HTPP system was field

424   deployed. Most days had high temperature extremes above 32° (Figure S1), a threshold

425   temperature above which lint yields sharply decrease (Schlenker and Roberts 2009). Among the

426   three field seasons, there were statistically significant differences ($P < 0.05$) for air temperature

427   (°C), relative humidity (%), vapor pressure deficit (kPa), precipitation (mm), and

428   evapotranspiration (mm) but not for solar radiation (MJ/m^2) (Table S1). The results from

429   analyzing meteorological data from specific days on which measurements were taken by the

430   HTPP system (Table S2) revealed that relative humidity, air temperature, and vapor pressure

431   deficit were significantly different ($P < 0.01$) (Table S1). With the exception of monsoon rainfall

432   events on days 228 and 234 (Julian calendar) of the 2012 field season, precipitation was

433   minimal. These two events led to saturated soil conditions that prevented the use of the HTPP

434   system for these two weeks. Although years differed for most environmental parameters, the hot,

435   arid environment of central Arizona consistently provided conditions conducive to imposing heat

436   and drought stress on the TM-1×NM24016 RIL population.

437   **HTPP of canopy traits**

438   We used the HTPP system to evaluate how four plant canopy phenotypes of the TM-

439   1×NM24016 RIL population responded to high temperature and water deficit under two

440   managed irrigation regimes, WW and WL, at different times of day from the early reproductive

441   through boll and fiber maturation phases in 2010-12. The multiple times throughout the day in

442   which measurements of canopy temperature, NDVI, height, and LAI were taken by the HTPP

443   system or calculated from post-processed data related to early morning (0700 or 0900),

444   midmorning (1000 or 1100), afternoon (1300), and/or late afternoon (1500) within a maximum

445   of 20 days. Indicative of an elicited physiological response, WL plots exhibited a warmer

446   average canopy temperature compared to WW plots across the three years (Figure S2), with

447   irrigation regime significant ($P < 0.05$ to 0.0001) for canopy temperature for 16 of the 19 days

448   (Table S3). In addition, time of day ($P < 0.05$ to 0.0001) was significant for 18 of 19 days (Table

449   S3). Illustrative of the rapid response that canopy temperature has to stomatal closure under

450   limiting soil moisture, high air temperature and vapor pressure deficit, early morning

451   measurements (0700 MST) of canopy temperature were often similar between irrigation regimes,

452   but as time progressed during the day there was a more rapid change in canopy temperature for

453   WL plots relative to WW plots (Figure 1, Figure S3, Figure S4, Figure S5, Table S4, Table S5,

454   Table S6).

455   The WW plots had higher NDVI than WL plots (Figure S6), with the effect of irrigation

456   regime being significant ($P < 0.05$ to 0.0001) for 15 out of 20 days across the three years (Table

457   S7). In contrast to canopy temperature, time of day was significant only 5 of 20 days for

458   NDVI—a trait that is less temporally responsive to environmental stress (Table S7). Inverse to

459   canopy temperature, we found that NDVI for WL plots generally decreased over the course of a

460   day whereas NDVI for WW plots either remained constant or increased slightly (Figure 1, Figure

461   S7, Figure S8, Figure S9, Table S8, Table S9, Table S10). Similar to what was observed for

462   Pima cotton (Andrade-Sanchez et al. 2014), this change in NDVI for WL plots was due to leaf

463   wilting from loss in turgidity, causing changes to the canopy geometry that resulted in lower

464   reflective values due to greater soil reflectivity in the instrument's field of view. It is likely that

465   the slight increase in NDVI for WW plots arose from a phenomenon known as diaheliotropism

466   in which leaves track the movement of the sun (Lang 1973; Ehleringer and Hammond 1987).

467   The height of the canopy for the TM-1×NM24016 RIL population from 2011 and 2012

468   (measured on a total of 14 days) displayed the expected pattern of WW plots having taller

469   canopies than the WL plots (Figure 1, Figure S10) and a change in height representing

470   incremental plant growth over the season (Figure S11, Figure S12, Table S11, Table S12).

471   Irrigation regime effects for 2012 followed an anticipated trend in which early season

472   measurements were either not significant or only slightly significant ($P < 0.05$, Table S13) until

473   midseason when they were all highly significant ($P < 0.0001$). In contrast, treatment effects for

474   2011 were more variable, in that some early season measurements were highly significant (day

475   202, $P < 0.0001$) followed by a day where the difference between irrigation regimes was not

476   significant (day 216). This variability likely resulted from clogged irrigation tape and emitters

477   which prevented uniform water distribution across plots. In order to reestablish experimental

478   field conditions, equal furrow irrigation was applied which attenuated the height differences

479   between irrigation regimes, but WW plots were still taller than WL plots. In general, time of day

480   was not significant; however, time of day was significant toward the end of the 2012 season

481   (days 222 -258) due to either severe wilting or the weight of bolls causing less turgid plants in

482   WL plots to lodge.

483   To gain further insight into the whole canopy response (Gutierrez et al. 2012; Thorp et al.

484   2015), we estimated LAI based on canopy NDVI and height from 2011 and 2012. As expected,

485   the WW plots had higher LAI than WL plots in both years (Figure S13). Additionally, LAI

486   exhibited a curvilinear trend across the growing season, reflecting progressive plant development

487   and biomass accumulation (Figure S14, Figure S15). Time of day was not significant for 12 of

488   14 days, whereas the effect of irrigation regime was significant ($P < 0.05$ to 0.0001) for 13 of 14

489   days (Table S14). Consistent with canopy NDVI, WW plots were able to maintain higher values

490   of LAI over the course of a day. However, WL plots experienced a gradual decrease in LAI that

491   was likely from a continuing increase in leaf wilting that concomitantly lowered NDVI (Figure

492   1, Table S15, Table S16).

493   In general, all HTPP canopy traits were highly heritable (average $\hat{H}^2$ of 0.87) under both

494   irrigation regimes across the three years (Figure S16, Figure S17, Figure S18, Figure S19, Table

495   S17, Table S18, Table S19, Table S20). The average of broad-sense heritability estimates for

496   both irrigation regimes across years for canopy temperature, NDVI, canopy height, and LAI

497   were 0.80, 0.86, 0.92, and 0.93, respectively, with the highest estimate ($\hat{H}^2 = 0.98$) calculated for

498   NDVI under WL conditions in 2011 and 2012. However, there were days in which estimates

499   were low and nearly zero in one instance ($\hat{H}^2 = \sim0$ for NDVI under both WW and WL, day 188,

500   2011). The days on which the HTPP traits had relatively lower estimates of heritability typically

501   occurred earlier in the season prior to canopy closure when exposed soil likely influenced the

502   proximally sensed measurements. In addition, the increased environmental variance in

503   heritability estimates for canopy temperature in 2011 (Figure S16) under WW conditions was

504   likely due to the eventually resolved irrigation issues encountered with clogged drip irrigation

505   tape and emitters.

506   **Agronomic, Fiber, and Physiological Traits**

507   Lint yield, boll size, and seed per boll all exhibited large genotypic and irrigation regime effects

508   ($P < 0.0001$) when assessed over the three growing seasons (Table S21). As expected for

509   complex traits, lint yield displayed a significant genotype-by-irrigation regime interaction ($P <$

510   0.001) as did seed per boll ($P < 0.05$), thus highlighting their responsiveness to the water deficit

511   treatment. However, broad-sense heritabilities for these three agronomic traits were high across

512   the three years and two irrigation regimes, with estimates ranging from 0.66-0.81 (Table 1).

513   Similar to canopy height, the irrigation regime effect for plant height, which was manually

514   measured multiple times throughout each field season, was generally found to be significant ($P <$

515   0.05 to < 0.0001; Table S22), with WW plots being taller than WL plots (Figure S20, Figure

516   S21, Figure S22, Figure S23, Table S23, Table S24, Table S25). The range of values for plant

517   height were larger than those for canopy height, with plant height values ~30% larger than those

518 for canopy height. Estimates of broad-sense heritability for plant height on different days ranged

519 from 0.48 to 0.89 for WW and WL conditions (Figure S24, Table S26).

520   The five fiber quality traits investigated in this study, fiber elongation, micronaire,

521 strength, length (upper half mean), and uniformity, exhibited extensive phenotypic variation and

522 high heritability across the three years (average $\hat{H}^2$ of 0.84 across both irrigation regimes). Of

523 these five traits, fiber strength under WW conditions had the lowest estimate of broad-sense

524 heritability ($\hat{H}^2 = 0.79$), while fiber elongation and uniformity under WL conditions had the

525 highest estimate ($\hat{H}^2 = 0.88$). With the exception of fiber length (irrigation regime; $P < 0.0001$),

526 which has a known response to water deficit (Allen and Aleman 2011), and micronaire

527 (genotype-by-irrigation regime; $P < 0.05$), none of the fiber traits showed a significant irrigation

528 regime or genotype-by-irrigation regime interaction (Table S21). Taken together, the relatively

529 high heritabilities and lack of environmental perturbation suggest that variation for these fiber

530 traits is mostly under the control of genetic effects.

531   The three physiological traits measured in this study, leaf ABA concentration, sugar

532 concentration, and carbon isotope discrimination (CID), showed genotypic differences ($P < 0.05$

533 to < 0.0001, Table S21), but did not vary with irrigation regime ($P > 0.05$). However, when these

534 traits were analyzed within a year, there were often significant differences between irrigation

535 regimes (Table S27). The estimated broad-sense heritabilities for these traits, averaged across

536 irrigation regimes, were 0.19, 0.31, and 0.16 for ABA, CID, and leaf sugar concentration,

537 respectively. The relatively lower broad-sense heritability estimates for these traits in

538 combination with the variable treatment effects observed for individual years highlight the

539 sensitivity of these physiological traits to environmental factors.

540 **Phenotypic correlations**

541   We investigated the degree of relationship between traits by calculating pairwise correlation

542   coefficients (Pearson's r) between all traits under both WL and WW conditions (File S4, an

543   additional set of BLUEs on a yearly basis were generated for the non-HTPP traits). In assessing

544   the strength of correlations between the HTPP and physiological traits, only CID was found to

545   consistently have a significant correlation ($r = 0.35$ to 0.40; $P < 0.001$) with canopy height on five

546   separate days in 2011 under WW conditions at a Bonferroni correction of 5%. With the

547   exception of canopy temperature, most of the fiber traits did not significantly covary with any of

548   the HTPP traits on any one day across the three years. Fiber elongation was significantly

549   correlated with canopy temperature during boll maturation for 2010 WL, 2011 WW, and 2012

550   WL treatments, with a maximum correlation of -0.35 ($P < 0.05$) under WL conditions in 2012.

551   Although not significant at a Bonferroni correction of 5%, micronaire tended to have a weak,

552   negative correlation ($r < 0.30$) across years (maximum r of -0.31 in 2010) with canopy

553   temperature.

554   The correlations of HTPP traits with boll size and lint yield were stronger and more

555   consistent than observed for physiological and fiber quality traits. Significant ($P < 0.05$),

556   negative correlations were found for boll size with canopy temperature ($r = -0.38$ to -0.35),

557   canopy height ($r = -0.40$ to -0.35), and LAI ($r = -0.40$ to -0.35) in both WL and WW irrigation

558   regimes in 2011, although correlations were strongest for the WL regime. The strongest

559   correlations between boll size and canopy temperature were identified early in the season

560   (flowering/peak bloom), whereas boll size was most strongly correlated with canopy height and

561   LAI during the fiber development and elongation phase. We also detected moderately strong

562   correlations for lint yield with canopy temperature and NDVI for both WL and WW plots.

563   Significant correlation values ($P < 0.05$) between lint yield and NDVI ranged from 0.35 to 0.61

564 for the three years under both irrigation regimes, while for canopy temperature the values ranged

565 from -0.42 to -0.62. When fitting a non-linear curve to lint yield and canopy temperature for the

566 time point identified with the strongest correlation each year, the fit of the curve (r^2) ranged from

567 0.11 to 0.30 (Figure 2). In contrast to boll size, the strongest correlations between lint yield and

568 canopy temperature were observed at flowering/peak bloom (Table S28).

569   When investigating the degree of relationship between HTPP traits, canopy temperature

570 was found to have significant, negative correlations ($P < 0.05$ to < 0.0001) with NDVI, canopy

571 height, and LAI over all three years for both irrigation regimes. In general, the strongest

572 correlations between canopy temperature and these three canopy HTPP traits was observed in the

573 afternoon at peak physiological stress irrespective of plant developmental stage. In addition,

574 significant, positive correlations ($P < 0.05$ to < 0.0001) were observed between all pairwise

575 comparisons of canopy height, NDVI, and LAI, but the strength of the association varied across

576 the different developmental phases of plant growth. Interestingly, we found that the strength of

577 the correlations between measurements of a canopy trait within a plant developmental stage were

578 stronger than between stages. This is best exemplified by canopy temperature under both

579 irrigation regimes in 2011 where there is a distinct pattern to the strength of correlations that has

580 a strong relationship with plant phenology (Figure 3, File S4).

581 **QTL identification**

582 We mapped QTL controlling phenotypic variation for the HTPP and non-HTTP traits in the TM-

583 1×NM24016 RIL population. The complete results of QTL mapping results are presented in

584 Supporting Information. When conducting the QTL analysis for HTPP traits, each day was

585 analyzed independently but mapping was performed across multiple time points within a day.

586 Through the implementation of this approach, we generally identified concordant QTL in terms

587   of genomic position associated with HTPP traits across individual days and multiple years in

588   both the WL and WW treatments. In total, we identified 14, 15, 14, and 16 QTL for canopy

589   temperature, NDVI, canopy height and LAI, respectively, at an experiment-wise Type I error

590   rate of $\alpha = 0.05$, with phenotypic variance explained (PVE) by each QTL ranging from 4.35 to

591   12.42%.

592   For canopy temperature, the 14 QTL were distributed across 13 chromosomes with one

593   of them detected under WW conditions only (Table S29). Of these 14 QTL, four of them were

594   detected in all three years under both WL and WW treatments. The total number of days on

595   which these four QTL were identified ranged from six to 14 (canopy temperature was collected

596   on a total of 19 days across the three years). These four QTL were located on the following

597   chromosomes: A08; A09; D10; and D12. The two QTL located on chromosomes D10 and D12

598   had an average PVE of 6.36% and 8.59% and a maximum PVE of 13.48% and 14.77%,

599   respectively. In addition, the average additive allelic effect estimates of the D10 and D12 QTL

600   were 0.30 and -0.29°, respectively. The QTL on A08 was detected on 12 of the 19 days. This

601   consistent detection was likely due to its relatively large allelic effect estimate, with estimated

602   average and maximum effects of -0.34° (7.59% PVE) and -0.62° (15.17% PVE), respectively.

603   Interestingly, canopy temperature QTL identified on chromosomes A09 and A13 colocalized

604   with QTL identified for leaf CID and ABA concentration, respectively, that were detected under

605   WL conditions. The genomic interval for the CID QTL on chromosome A09 contained a

606   candidate gene (Gene ID: Gh_A13G0355) previously described in *Arabidopsis thaliana* as a

607   member of the *AtDi19* gene family implicated in dehydration and abiotic stress response (Milla

608   et al. 2006). In addition, the genomic interval containing the ABA QTL on chromosome A13

609   included a candidate gene (Gene ID: Gh_A13G0355) identified in *A. thaliana* as an abscisic acid

610 response element (ABRE) binding factor implicated in stress responsive ABA signaling (Kang et

611 al. 2002; Kim et al. 2004).

612   The 15 QTL identified for NDVI were located across 14 chromosomes, and of these,

613 three QTL were associated with only a single irrigation regime (Table S30). Notably, two-thirds

614 of the 15 QTL were shared based on overlapping genomic positions with those detected for

615 canopy temperature. Given the inverse phenotypic correlation between NDVI and canopy

616 temperature, it was not surprising that the associated allelic effect estimates for the shared QTL

617 were in opposing directions. Of these shared QTL, the QTL identified on chromosome A08

618 exhibited major control of variation for NDVI. Specifically, this QTL, which had an average

619 PVE of 10.42%, was detected on 19 of the 20 days on which spectral data were collected across

620 the three years.

621   We identified 14 QTL that controlled variation for canopy height over the three growing

622 seasons (Table S31). As expected, six of these QTL were shared with plant height (Table S32)

623 and to which canopy height was also strongly correlated at the phenotypic level ($r = 0.46$ to 0.91,

624 $P < 0.0001$). This result suggests a moderate to high degree of concordance between the two

625 measurement approaches. In addition, the results from QTL mapping of canopy height were

626 comparable to those of LAI, with the genomic positions of 12 QTL shared between the two traits

627 (Table S31, Table S33). The four QTL not concordant between canopy height and LAI, however,

628 were shared between canopy height and NDVI. These findings were not unexpected given that

629 the calculation of LAI was predominantly based on canopy height and NDVI.

630   The mapping of QTL for agronomic and fiber quality traits identified a total of 22 QTL

631 that mapped to 11 chromosomes and of which 18 QTL were unique among traits and irrigation

632 regimes (Table S34). We identified eight QTL for lint yield with allelic effects values ranging

28

633   from -80.79 (17.85% PVE) to 67.34 kg ha^{-1} (14.76% PVE). Of these QTL, the QTL on D01

634   mapped to the same genomic location as that of QTL for canopy temperature and NDVI,

635   suggesting at least a partly shared genetic basis between these two HTPP canopy traits and lint

636   yield. Lint yield is very likely to have even more QTL shared with canopy temperature and

637   NDVI, but the small sample size of 95 RILs did not provide sufficient statistical power to

638   identify QTL with small to intermediate effects for a polygenic trait such as lint yield (Xu 2003).

639   Regardless, further supporting this association, a boll size QTL on chromosome A05 co-

640   localized with QTL detected for canopy temperature, NDVI, canopy height, and LAI under both

641   irrigation regimes. With respect to the fiber quality traits, none of the identified QTL were shared

642   with those detected for HTPP traits, although we only detected a few unique QTL for fiber

643   elongation, uniformity and micronaire.

644   **Patterns of identified QTL**

645   The HTPP system enabled collection of phenotypic data throughout the season that afforded us

646   the opportunity to assess QTL patterns (i.e., presence vs. absence of significant QTL) within and

647   across years as well as between different irrigation regimes. Of all the HTPP traits, canopy

648   temperature exhibited the most dynamic QTL patterns. Exemplifying this dynamism, QTL

649   identified on chromosomes A09, A12, D04, and D12 showed a strong temporal pattern, varying

650   in frequency of identification from six to 14 days (Figure 4, Table S29). In 2011 and 2012, the

651   canopy temperature QTL on chromosome A12 was not detected until day 216 after which point

652   it was continually detected until approximately day 250 under both irrigation regimes. Similar

653   patterns were also observed for the two canopy QTL on chromosomes D04 and D12, which

654   suggests that all three QTL initiate expression at boll development and continue throughout the

655   fiber elongation and maturation phase. Finally, the QTL on chromosome A09 was identified

656 predominately under WL conditions at approximately midseason with its effects diminishing by

657 day ~250 in 2011 and 2012.

658   The patterns of identified QTL for NDVI were different from canopy temperature in that

659 there was less within season variability. The majority of NDVI QTL were either detected for the

660 duration of the season or beginning midseason at approximately day 220, coinciding with the

661 boll development and fill phase in 2011 and 2012. However, the preferential identification of

662 QTL under a specific irrigation regime was still observed, especially three QTL on chromosomes

663 A10, D06, and D12 (Figure S25). The QTL on chromosome A10, which was detected on eight

664 different days across the three years, displayed the most dramatic specificity as its expression

665 was nonexistent for the WW treatment. The expression of QTL on chromosomes D06 and D12

666 were exclusively associated to the WW treatment, with the D06 and D12 QTL detected in 2011

667 and 2012 on 12 and 11 different days, respectively. With respect to QTL patterns for canopy

668 height and LAI, neither trait displayed strong temporal variability nor irrigation regime

669 specificity as most QTL were repeatedly detected from the beginning of data collection

670 throughout the growing season under both WW and WL conditions (Figures S26, S27).

671   **DISCUSSION**

672   The genetic improvement of cotton for yield and fiber quality traits is largely dependent

673 on identifying and understanding key genes and alleles responsible for enhanced productivity

674 under limiting environmental conditions. Central to this challenge is the ability to collect

675 phenotypic data on experimental populations under real-world production conditions

676 encountered throughout the growing season. In that light, we demonstrated the use of an HTPP

677 system to measure canopy traits on a RIL population grown under contrasting irrigation regimes

678 in a hot, arid environment. Through the analysis of data collected by the HTPP system, we

679 mapped QTL controlling the temporal response of canopy traits to heat and drought stress, and

680 demonstrated how these HTPP traits related to agronomic, physiological and fiber quality traits.

681 To the best of our knowledge, this is the first study using field-based HTPP to investigate the

682 genetic basis of phenotypic responses to heat and drought stress in a genetic mapping population

683 over multiple growing seasons.

684   Paramount to the success of studying traits that change in response to environmental

685 stimuli is the ability to collect data from experimental plots at multiple time points per day, as

686 this provides a way to quantify the physiological processes underlying dynamic phenotypes. The

687 temporal effects of stomatal closure can be seen by assessing the change in canopy temperature

688 over the course of a day (Figure 1). Day 222 from 2012 was one of the more severe days in terms

689 of high air temperature (maximum temperature of 37.76°) and co-occurring high vapor pressure

690 deficit (VPD, 4.94 kPa). Early in the morning plant canopy temperatures were approximately

691 equivalent but as the day progressed the two treatments diverged drastically as WW plots were

692 able to maintain lower canopy temperatures unlike the drought stressed, WL plots. At peak

693 stress, occurring around 1300 MST, the difference in temperature between the two irrigation

694 regimes was ~10°, and WL plots had an average canopy temperature of 45°. The elevated

695 canopy temperatures of WL plots is indicative of stomatal closure, mediated through ABA

696 signaling, which is one of the primary plant responses to water deficit and serves as a mechanism

697 to conserve water resources (Ackerson 1980; Taiz and Zeiger 2006). The closure of stomata

698 leads to elevated canopy temperatures because plants are no longer able to use evaporative

699 cooling, via increased transpiration, to modulate thermal homeostasis (Carmo-Silva et al. 2012;

700 Radin et al. 1994; Burke and Wanjura 2010). A QTL identified for ABA concentration, which

701 co-located with a QTL associated with canopy temperature, supports an expected relationship

702   between stomatal conductance and canopy temperature. Additionally, the co-localization of CID

703   and canopy temperature QTL illustrates a shared genetic relationship between these two

704   physiological traits. The positive allelic effects for both QTL imply a reduction in the

705   preferential usage of C^{12} over C^{13} along with a concomitant increase in canopy temperature,

706   which would result from limited gas exchange between leaf intercellular airspaces and the

707   atmosphere due to stomatal closure (Fischer et al. 1998; Farquhar et al. 1982).

708   The high canopy temperatures observed in the WL treatment led to heat stress and its

709   subsequent effects, which likely included reduced flower fertility and boll set in addition to

710   diminished photosynthetic capacity and eventual overall productivity (Dabbert and Gore 2014;

711   Taiz and Zeiger 2006; Carmo-Silva and Salvucci 2012). The repeatedly observed inverse

712   relationship between canopy temperature and lint yield, an indicator of overall plant productivity,

713   observed during flowering/peak bloom highlights the salient point that higher leaf transpiration

714   rate provides a protective micro-environment for crucial reproductive organs. This adaptive

715   advantage to cope with unfavorable environmental conditions provides a benefit in terms of lint

716   yield when grown under sufficient irrigation in a hot, arid environment (Figure 2), as more

717   fertilized flowers develop into bolls that are retained through maturation and harvest.

718   The phenotypic effects of drought and heat stress can further manifest themselves by

719   altering the orientation of leaves that constitute the canopy geometry. Our results show that for

720   WL plots, NDVI decreases due to leaf wilting over the course of a day (Figure 1) likely in

721   response to low leaf water potential during drought stress (Carmo-Silva et al. 2012). The

722   progressive decrease in NDVI tracks directly with the increase in canopy temperature, albeit

723   inversely, over the same time frame. In comparison, NDVI in the WW plots remained high over

724   the course of a day, because canopy geometry was more stable. This was because the leaves of

725　plants under WW conditions were at higher turgor pressure and could maintain a perpendicular

726　orientation to incoming light, but under WL conditions the water potential of leaves was reduced

727　causing a loss of turgor pressure that led to wilting (Zhang et al. 2010). Because the angular

728　distribution of leaf area in the canopy was altered to expose more soil in the sensor's field of

729　view under WL conditions, the amount of near-infrared light reflected was decreased, leading to

730　lower NDVI values. At the whole plant level, LAI (calculated as a function of canopy height and

731　NDVI) followed the same trend of decreasing values for the WL irrigation regime over time with

732　non-stressed, WW plots not changing. Taken together, these results support the hypothesis that

733　the imposed heat and drought stress resulted in in elevated canopy temperature and wilting in a

734　time dependent manner.

735　　　The use of an HTPP system provided us the unique ability to assess variation in canopy

736　traits over plant developmental stages within and across growing seasons. The canopy

737　temperature correlation values presented in Figure 3 (observed for the other HTPP traits as well)

738　demonstrate how the different stages of cotton plant development can be defined by their

739　phenotypic correlations as well as their associated temporal patterns of QTL expression.

740　Although a mapping population of 95 RILs is underpowered for QTL analysis, which limits the

741　ability to detect QTL of small to intermediate effect (Xu 2003), its use in this study did not

742　compromise the consistent detection of large effect QTL across plant developmental stages.

743　Canopy temperature exhibited the most dynamic QTL patterns with notable QTL located on

744　chromosomes A05, A09, A12, and D04 that initiated expression at approximately day 216,

745　coinciding with the beginning of boll development and fill (Figure 4). Similar to canopy

746　temperature, QTL associated with NDVI on chromosomes A05, A12, A13, and D04 were

747　detected at approximately day 220. For the remainder of NDVI QTL identified in addition to

33

748 those detected for canopy height and LAI, distinct temporal patterns of QTL expression were not

749 as evident. This is most likely due to the inherent relationship between these traits and plant

750 biomass, a property that changes slowly in response to environmental stimuli. Taken together,

751 these findings validate the need for continued phenotyping throughout the season in order to

752 develop a complete picture of abiotic stress response, as no single time point is representative of

753 the diverse physiological processes occurring in the crop. This study also demonstrates the

754 successful implementation of mapping QTL with variable temporal expression. We would have

755 most likely missed capturing these genetic signals, especially for canopy temperature, had

756 traditional single-time point data collection methods been employed.

757   With respect to applied plant breeding, our results illustrate how HTPP would be a useful

758 tool for evaluating large breeding populations grown under abiotic stress conditions, allowing for

759 the selection of superior genotypes having a favorable array of QTL alleles. We detected

760 significant correlations between HTPP canopy and agronomic traits, with the strength of

761 association dependent on growth stage. For canopy temperature and NDVI, the strongest

762 correlations (r^2) with lint yield were observed during flowering/peak bloom (Figure 2), a growth

763 stage that significantly impacts yield but is also highly susceptible to abiotic stress (Burke and

764 Wanjura 2010; Oosterhuis and Snider 2011; Dabbert and Gore 2014). The QTL on A08, whose

765 allelic effect decreased canopy temperature and maintained NDVI (i.e., less wilting) during this

766 developmental time and throughout the season, provides an ideal example of QTL that could be

767 selected for to mitigate the effects of unfavorable conditions at critical phenological stages.

768 Although bolls per unit area is the component trait having the strongest relationship with lint

769 yield (Pettigrew 2004), boll size—another trait that has a significant association with lint

770 yield—was also correlated with canopy temperature during flowering/peak bloom. However,

771 boll size also exhibited significant correlations with canopy height and LAI during fiber

772 development and elongation, a key time for fiber quality determination that is also sensitive to

773 high temperatures (Allen and Aleman 2011). For both lint yield and boll size, the observed

774 correlations with HTPP canopy traits were generally the strongest under WL conditions. Given

775 the significant correlations of lint yield and boll size with HTPP canopy traits, the additional use

776 of these HTPP traits as indirect selection criteria in water-limited environments could provide

777 more genetic gain than selection on lint yield and its components alone (Bernardo 2010).

778 **CONCLUSION**

779 The phenotyping of plant populations for the study of key agronomic, fiber quality, and

780 physiological traits in cotton has always been a challenge, and with ever increasing population

781 sizes for cotton (Patterson 2012; Abdurakhmonov et al. 2014; Tyagi et al. 2014), will remain so

782 unless HTPP tools become more prevalent and advanced. The implementation of an HTPP

783 system in conjunction with traditional phenotyping enabled us to study and characterize the

784 response of 95 RILs to the abiotic stresses of heat and drought. Our results demonstrate the

785 ability to map QTL controlling the dynamic response of canopy traits to abiotic stress and also

786 revealed the temporal nature of QTL expression patterns. Longitudinal phenotypic assessment of

787 canopy traits also provided insight as to which canopy traits are potentially most predictive of

788 lint yield at specific stages of plant development. In summary, our work illustrates how field-

789 based HTPP is a potentially powerful tool to better exploit genomics data for the genetic

790 improvement of crops which will greatly assist in meeting the challenges facing plant breeding in

791 the 21st century.

792 **ACKNOWLEDGEMENTS**

801 **REFERENCES**

802 Abdurakhmonov, I. Y., A. Abdullaev, Z. Buriev, S. Shermatov, F. N. Kushanov *et al.*, 2014

803   *Cotton Germplasm Collection of Uzbekistan*.

804 Ackerson, R. C., 1980 Stomatal response of cotton to water stress and abscisic acid as affected

805   by water stress history. *Plant Physiology* 65: 455-459.

806 Allen, R. D., and L. Aleman, 2011 Abiotic stress and cotton fiber development, pp. 153 in *Stress*

807   *Physiology in Cotton*, edited by D. M. Oosterhuis. The Cotton Foundation, Cordova,

808   Tennessee.

809 Allen, R. G., L. S. Pereira, D. Raes, and M. Smith, 1998 Crop evapotranspiration - guidelines for

810   computing crop water requirements - FAO irrigation and drainage paper 56. Food and

811   Agriculture Organization of the United Nations, Rome.

812 Anderson, M. J., and C. J. F. Braak, 2003 Permutation tests for multi-factorial analysis of

813   variance. *Journal of Statistical Computation and Simulation* 73 (2): 85-113.

814 Andrade-Sanchez, P., M. A. Gore, J. T. Heun, K. R. Thorp, A. E. Carmo-Silva *et al.*, 2014

815   Development and evaluation of a field-based high-throughput phenotyping platform.

816   *Functional Plant Biology* 41: 69-79.

817 Araus, J. L., and J. E. Cairns, 2014 Field high-throughput phenotyping: the new crop breeding

818   frontier. *Trends in Plant Science* 19 (1): 52-61.

819 Belsley, D. A., E. Kuh, and R. E. Welsch, 2004 *Regression Diagnostics: Identifying Influential*

820   *Data and Sources of Collinearity*. Hoboken, NJ: John Wiley & Sons.

821 Bernardo, R., 2010 *Breeding for Quantitative Traits in Plants*. Woodbury, Minnesota: Stemma

822   Press.

823   Brown, P. W., 1989 Accessing the Arizona Meteorological Network (AZMET) by Computer in

824   *Extension Report No. 8733*. University of Arizona, Tucson.

825   Burke, J. J., and D. F. Wanjura, 2010 Plant response to temperature extremes, pp. 123-124 in

826   *Physiology of Cotton*, edited by J. M. Stewart, D. M. Oosterhuis, J. J. Heitholt and J. R.

827   Mauney. Springer, New York.

828   Busemeyer, L., A. Ruckelshausen, K. Moller, A. E. Melchinger, K. V. Alheit *et al.*, 2013

829   Precision phenotyping of biomass accumulation in triticale reveals temporal genetic

830   patterns of regulation. *Sci. Rep.* 3.

831   Camacho, C., G. Coulouris, V. Avagyan, N. Ma, J. Papadopoulos *et al.*, 2009 BLAST+:

832   architecture and applications. *BMC Bioinformatics* 10 (421): 1-9.

833   Campos, H., M. Cooper, J. E. Habben, G. O. Edmeades, and J. R. Schussler, 2004 Improving

834   drought tolerance in maize: a view from industry. *Field Crops Research* 90 (1): 19-34.

835   Carmo-Silva, A. E., M. A. Gore, P. Andrade-Sanchez, A. N. French, D. J. Hunsaker *et al.*, 2012

836   Decreased CO_2 availability and inactivation of Rubisco limit photosynthesis in cotton

837   plants under heat and drought stress in the field. *Environmental and Experimental Botany*

838   83: 1-11.

839   Carmo-Silva, A. E., and M. E. Salvucci, 2012 The temperature response of CO2 assimilation,

840   photochemical activities and Rubisco activation in Camelina sativa, a potential bioenergy

841   crop with limited capacity for acclimation to heat stress. *Planta* 236 (5): 1433-1445.

842   Chaves, M. M., J. P. Maroco, and J. Pereira, 2003 Understanding plant responses to drought -

843   from genes to the whole plant. *Functional Plant Biology* 30 (3): 239-264.

844   Churchill, G. A., and R. W. Doerge, 1994 Empirical threshold values for quantitative trait

845   mapping. *Genetics* 138 (3): 963-971.

846   Cotton Inc., 2015 Monthly economic letter, September 2015. Cotton Incorporated.

847   Dabbert, T. A., and M. A. Gore, 2014 Challenges and perspectives on improving heat and

848   drought stress resilience in cotton. *Journal of Cotton Science* 18: 393-409.

849   Davey, J. W., P. A. Hohenlohe, P. D. Etter, J. Q. Boone, J. M. Catchen *et al.*, 2011 Genome-

850   wide genetic marker discovery and genotyping using next-generation sequencing. *Nat*

851   *Rev Genet* 12 (7): 499-510.

852   Ehleringer, J. R., and S. D. Hammond, 1987 Solar tracking and photosynthesis in cotton leaves.

853   *Agricultural and Forest Meteorology* 39 (1): 25-35.

854   Farquhar, G., M. O'Leary, and J. Berry, 1982 On the relationship between carbon isotope

855   discrimination and the intercellular carbon dioxide concentration in leaves. *Functional*

856   *Plant Biology* 9 (2): 121-137.

857   Farquhar, G. D., J. R. Ehleringer, and K. T. Hubick, 1989 Carbon isotope discrimination and

858   photosynthesis. *Annual review of plant biology* 40 (1): 503-537.

859   Fischer, R. A., D. Rees, K. D. Sayre, Z. M. Lu, A. G. Condon *et al.*, 1998 Wheat yield progress

860   associated with higher stomatal conductance and photosynthetic rate, and cooler

861   canopies. *Crop Science* 38 (6): 1467-1475.

862   Furbank, R. T., and M. Tester, 2011 Phenomics – technologies to relieve the phenotyping

863   bottleneck. *Trends in Plant Science* 16 (12): 635-644.

864   Gilmour, A. R., B. J. Gogel, B. R. Cullis, and R. Thompson, 2009 *ASReml User Guide Release*

865   *3.0*. Hemel Hempstead, UK: VSN International Ltd.

866   Gore, M. A., D. D. Fang, J. A. Poland, J. Zhang, R. G. Percy *et al.*, 2014 Linkage map

867   construction and quantitative trait locus analysis of agronomic and fiber quality traits in

868   cotton. *The Plant Genome* 7 (1): 1-10.

869   Gore, M. A., R. G. Percy, J. Zhang, D. D. Fang, and R. G. Cantrell, 2012 Registration of the TM-

870   1/NM24016 cotton recombinant inbred mapping population. *Journal of Plant*

871   *Registrations* 6 (1): 124-127.

872   Gutierrez, M., R. Norton, K. R. Thorp, and G. Wang, 2012 Association of spectral reflectance

873   indices with plant growth and lint yield in Upland cotton. *Crop Science* 52 (2): 849-857.

874   Holland, J. B., W. E. Nyquist, and C. Cervantes-Martinez, 2003 Estimating and interpreting

875   heritability for plant breeding: an update. *Plant Breeding Reviews* 22: 9-112.

876   Hunsaker, D. J., E. M. Barnes, T. R. Clarke, G. J. Fitzgerald, and J. P. J. Pinter, 2005 Cotton

877   irrigation scheduling using remotely sensed and FAO-56 basal crop coefficients. 48 (4).

878   Kang, J.-Y., H.-I. Choi, M.-Y. Im, and S. Y. Kim, 2002 Arabidopsis basic leucine zipper proteins

879   that mediate stress-responsive abscisic acid signaling. *The Plant Cell* 14: 343-357.

880   Kenward, M. G., and J. H. Roger, 1997 Small sample inference for fixed effects from restricted

881   maximum likelihood *Biometrics* 53 (3): 983-997.

882   Kim, S., J.-y. Kang, D.-I. Cho, J. H. Park, and S. Y. Kim, 2004 ABF2, an ABRE-binding bZIP

883   factor, is an essential component of glucose signaling and its overexpression affects

884   multiple stress tolerance. *The Plant Journal* 40: 75-87.

885   Lang, A. R. G., 1973 Leaf orientation of a cotton plant. *Agricultural Meteorology* 11: 37-51.

886   Li, H., G. Ye, and J. Wang, 2007 A modified algorithm for the improvement of composite

887   interval mapping. *Genetics* 175 (1): 361-374.

888   Li, S., J. Wang, and L. Zhang, 2015 Inclusive Composite Interval Mapping of QTL by

889   Environment Interactions in Biparental Populations. *PLoS ONE* 10 (7): e0132414.

890   Littell, R. C., G. A. Milliken, W. W. Stroup, R. D. Wolfinger, and O. Schabenberger, 2006 *SAS*

891   *for Mixed Models*. Cary, N.C.: SAS Institute.

892   Loka, D. A., D. M. Oosterhuis, and G. L. Ritchie, 2011 Water-Deficit Stress in Cotton, pp. 37-72

893   in *Stress Physiology in Cotton*, edited by D. M. Oosterhuis. The Cotton Foundation,

894   Cordova, TN.

895   Milla, M. A. R., J. Townsend, I.-F. Chang, and J. C. Cushman, 2006 The Arbidopsis *Atdi19* gene

896   family encodes a novel type of Cys2/His2 zinc-finger protein implicated in ABA-

897   independent dehydration, high-salinity stress and signaling pathways. *Plant Molecular*

898   *Biology* 61: 13-30.

899   Mulla, D. J., 2013 Twenty five years of remote sensing in precision agriculture: key advances

900   and remaining knowledge gaps. *Biosystems Engineering* 114 (4): 358-371.

901   National Agricultural Statistics Service, 2015 Crop Values 2014 Summary, pp. 31, edited by U.

902   S. D. o. Agriculture.

903   National Cotton Council of America, 2015 Cotton production costs and returns.

904   Neter, J., M. H. Kutner, C. J. Nachtsheim, and W. Wasserman, 1996 *Applied Linear Statistical*

905   *Models*. Boston: McGraw-Hill.

906   Oosterhuis, D. M., and J. L. Snider, 2011 High temperature stress on floral development and

907   yield of cotton, pp. 1-24 in *Stress Physiology in Cotton*, edited by D. M. Oosterhuis. The

908   Cotton Foundation, Cordova, Tennessee.

909   Patterson, A. H., 2012 Toward an exotic nested association mapping population set for upland

910   cotton. Cotton Inc. Project Summary 11-895.

911   Percy, R. G., R. G. Cantrell, and J. Zhang, 2006 Genetic variation for agronomic and fiber

912   properties in an introgressed recombinant inbred population of cotton. *Crop Science* 46:

913   1311-1317.

914   Pettigrew, W. T., 2004 Moisture deficit effects on cotton lint yield, yield components, and boll

915   distribution. *Agronomy Journal* 96 (2): 377-383.

916   R Core Team, 2014 R: A language and environment for statistical computing. R Foundation for

917   Statistical Computing, Vienna, Austria.

918   Radin, J. W., Z. Lu, R. G. Percy, and E. Zeiger, 1994 Genetic variability for stomatal

919   conductance in Pima cotton and its relation to improvements of heat adaptation.

920   *Proceedings of the National Academy of Sciences of the United States of America* 91

921   (15): 7217-7221.

922   Rizhsky, L., H. Liang, and R. Mittler, 2002 The combined effect of drought stress and heat shock

923   on gene expression in tobacco. *Plant Physiology* 130 (3): 1143-1151.

924   Schlenker, W., and M. J. Roberts, 2009 Nonlinear temperature effects indicate severe damages to

925   U.S. crop yields under climate change. *Proceedings of the National Academy of Sciences*

926   106 (37): 15594-15598.

927   Scotford, I. M., and P. C. H. Miller, 2004 Estimating tiller density and leaf area index of winter

928   wheat using spectral reflectance and ultrasonic sensing techniques. *Biosystems*

929   *Engineering* 89 (4): 395-408.

930   Setter, T. L., B. A. Flannigan, and J. Melkonian, 2001 Loss of kernel set due to water deficit and

931   shade in maize: Carbohydrate supplies, abscisic acid, and cytokinins. *Crop Science* 41:

932   1530-1540.

933   Setter, T. L., J. Yan, M. Warburton, J.-M. Ribaut, Y. Xu *et al.*, 2010 Genetic association

934   mapping identifies single nucleotide polymorphisms in genes that affect abscisic levels in

935   maize floral tissues during drought. *Journal of Experimental Botany* 62 (2): 701-716.

936   Taiz, L., and E. Zeiger, 2006 *Plant Physiology*. Sunderland, Massachusetts: Sinauer.

937   Thorp, K. R., M. A. Gore, P. Andrade-Sanchez, A. E. Carmo-Silva, S. M. Welch *et al.*, 2015

938   Proximal hyperspectral sensing and data analysis approaches for field-based plant

939   phenomics. *Computers and Electronics in Agriculture* 118: 225-236.

940   Tyagi, P., M. A. Gore, D. T. Bowman, B. T. Campbell, J. A. Udall *et al.*, 2014 Genetic diversity

941   and population structure in the US Upland cotton (*Gossypium, hirsutum* L.). *Theoretical*

942   *and Applied Genetics* 127 (2): 283-295.

943   USDA Economic Research Service, U.-E., 2015 Cotton & Wool.

944   White, J. W., P. Andrade-Sanchez, M. A. Gore, K. F. Bronson, T. A. Coffelt *et al.*, 2012 Field-

945   based phenomics for plant genetics research. *Field Crops Research* 133: 101-112.

946   Wu, R., and M. Lin, 2006 Functional mapping - how to map and study the genetic architecture of

947   dynamic complex traits. *Nat Rev Genet* 7 (3): 229-237.

948   Würschum, T., W. Liu, K. V. Alheit, M. R. Tucker, M. Gowda *et al.*, 2014 Adult plant

949   development in Triticale ($\times$ *Triticosecale Wittmack*) is controlled by dynamic genetic

950   patterns of regulation. *G3: Genes|Genomes|Genetics* 4 (9): 1585-1591.

951   Xu, S., 2003 Theoretical Basis of the Beavis Effect. *Genetics* 165 (4): 2259-2268.

952   Zhang, T., Y. Hu, W. Jiang, L. Fang, X. Guan *et al.*, 2015 Sequencing of allotetraploid cotton

953   (Gossypium hirsutum L. acc. TM-1) provides a resource for fiber improvement. *Nat*

954   *Biotech* 33 (5): 531-537.

955   Zhang, Y.-L., H.-Z. Zhang, M.-W. Du, W. Li, H.-H. Luo *et al.*, 2010 Leaf wilting movement can

956   protect water-stressed cotton (*Gossypium hirsutum* L.) plants against photoinhibition of

957   photosynthesis and maintain carbon assimilation in the field. *Journal of Plant Biology* 53:

958   52-60.

959

960 Table 1. Means, standard deviations, and ranges of best linear unbiased estimators (BLUEs) for traits evaluated for
961 the TM-1×NM24106 recombinant inbred line (RIL) population tested under two irrigation regimes, water-limited
962 (WL) and well-watered (WW) conditions, including parental lines and their midparent values. Estimates of broad-
963 sense heritability ($\hat{H}^2$) on an entry-mean basis are reported. Field trials were conducted from 2010 to 2012 at the
964 Maricopa Agricultural Center located in Maricopa, AZ.
965

Trait	Irrigation regime	Parents			RIL population				Heritability
		TM-1	NM24016	Midparent	Mean	Std. Dev	Min.	Max.	$\hat{H}^2$
ABA Conc.	WL	10.71	8.78	9.75	10.60	2.72	3.52	21.00	0.15
($p$mol/cm^2)	WW	6.99	6.76	6.88	7.00	1.89	3.18	11.39	0.23
Δ^{13}C	WL	20.28	19.72	20.00	20.25	0.28	19.59	20.80	0.31
(‰)	WW	20.50	20.13	20.32	20.49	0.31	19.47	21.14	0.30
Sugar conc.	WL	0.43	0.45	0.44	0.47	0.07	0.32	0.62	0.12
($u$mol/cm^2)	WW	0.40	0.41	0.41	0.41	0.07	0.27	0.71	0.19
Fiber elongation	WL	5.12	4.34	4.73	5.06	0.76	3.19	6.78	0.88
(%)	WW	5.26	4.27	4.77	5.10	0.77	3.26	6.92	0.87
Fiber micronaire	WL	5.09	4.30	4.70	4.36	0.57	3.19	5.75	0.83
(unit)	WW	5.04	4.38	4.71	4.37	0.56	3.09	5.73	0.80
Fiber uniformity	WL	82.69	84.17	83.43	82.81	0.94	80.11	84.90	0.88
(LUI)	WW	83.18	84.64	83.91	82.97	0.98	80.49	84.97	0.87
Fiber strength	WL	292.64	326.48	309.61	322.45	23.14	277.63	371.49	0.83
(kN m kg^{-1})	WW	290.09	327.16	308.63	320.49	21.67	276.46	391.59	0.79
Upper half mean	WL	1.11	1.18	1.15	1.13	0.05	0.99	1.25	0.81
(mm)	WW	1.13	1.19	1.16	1.14	0.06	0.99	1.27	0.83
Boll size	WL	4.73	2.50	3.62	3.29	0.56	2.15	4.66	0.70
(g boll^{-1})	WW	4.98	2.75	3.87	3.51	0.63	2.26	5.26	0.81
Lint yield	WL	667.25	325.00	496.13	402.61	135.15	178.33	920.16	0.71
(kg ha^{-1})	WW	890.60	454.48	672.54	523.55	173.80	138.34	1066.54	0.68
Seed per boll	WL	25.09	13.77	19.43	17.58	2.74	11.43	24.71	0.66
	WW	26.40	14.84	20.62	18.66	2.76	12.50	25.23	0.78

966

Table 2. Selective summary of quantitative trait loci (QTL) identified for HTPP canopy, agronomic, physiological, and fiber quality traits in the TM-1×NM24016 recombinant inbred line (RIL) population under two irrigation regimes, water-limited (WL) and well-watered (WW), at an experiment-wise Type I error rate of 5%. Marker positions are reported both in centimorgans (cM) on linkage groups and base pairs on respective chromosomes. The complete summary is included in Tables S29–S34.

Chromosome	LG	Left Marker	Left Marker Position (bp)	Left Marker Position (cM)	Right Marker	Right Marker Position (bp)	Right Marker Position (cM)	Interval Size	Traits[a]
A13	55	SNP0144	2,174,006	33.44	SNP0036	4,956,693	54.82	2,782,687	ABA, NDVI (55.00%), LAI (57.14%), CT (36.84%)
A09	32	SNP0003	70,791,307	38.53	SHIN-1542a	74,019,812	4.69	3,228,505	Δ^{13}C, CT (31.58%)
A05	74	SNP0029	3,926,888	0.00	SNP0159	5,616,973	24.03	1,690,085	Boll size, CHT (78.57%), NDVI (60.00%), LAI (92.86%), CT (42.11%)
A02	3	SHIN-0129b	40,970,937	11.53	DC40319b	41,271,319	12.81	300,382	Fiber Elongation
A11	44	SNP0179	84,855,703	5.32	SNP0140	89,784,339	1.12	4,928,636	Fiber Elongation
A11	91	BNL0625a	49,598,610	29.18	BNL2805a	49,637,476	28.68	38,866	Micronaire
D06	112	SNP0361	1,611,037	17.02	SNP0427	1,956,820	13.70	345,783	Micronaire
A06	19	SNP0154	9,290,498	12.87	SNP0070	9,440,198	13.80	149,700	Lint yield, CHT (78.57%)
D01	24	DPL0790a	70,178	0.00	CIR238a	3,374,597	16.60	3,304,419	Lint yield, NDVI (65.00%), CT (73.68%)
D09	99	C2-021a	21,552,954	2.32	SNP0259	21,636,248	0.00	83,294	Lint yield, Seed per boll
A06	21	SNP0426	2,294,776	20.03	SNP0146	2,540,030	9.23	245,254	NDVI (40.00%), LAI (35.71%), CT (36.84%)
A08	29	C2-003a	1,083,826	0.00	SNP0471	1,736,727	16.44	652,901	NDVI (95.00%), LAI (28.57%), CT (63.16%)
D12	54	SNP0331	993,024	0.00	SNP0425	1,432,973	18.45	439,949	CHT (64.29%), NDVI (55.00%), CT (73.68%)
A03	71	SHIN-0690a	2,612,135	0.00	SHIN-0727	2,644,274	10.86	32,140	CHT (57.14%), NDVI (35.00%), LAI (78.57%)
A12	45	MUSB1117a	3,597,960	9.76	SHIN-1413a	10,039,270	33.25	6,441,310	CHT (85.71%), NDVI (65.00%), LAI (85.71%)
D06	22	SNP0086	10,388,600	21.39	SNP0132	23,134,645	0.00	12,746,045	CHT (71.43%), NDVI (60.00%), LAI (85.71%), CT (21.05%)

a. Trait abbreviations: ABA, abscisic acid content; Δ^{13}C, carbon isotope discrimination; CHT, canopy height; NDVI, normalized difference vegetation index; LAI, leaf area index; CT, canopy temperature. Values listed in parentheses are the percentage of days on which the QTL were detected.
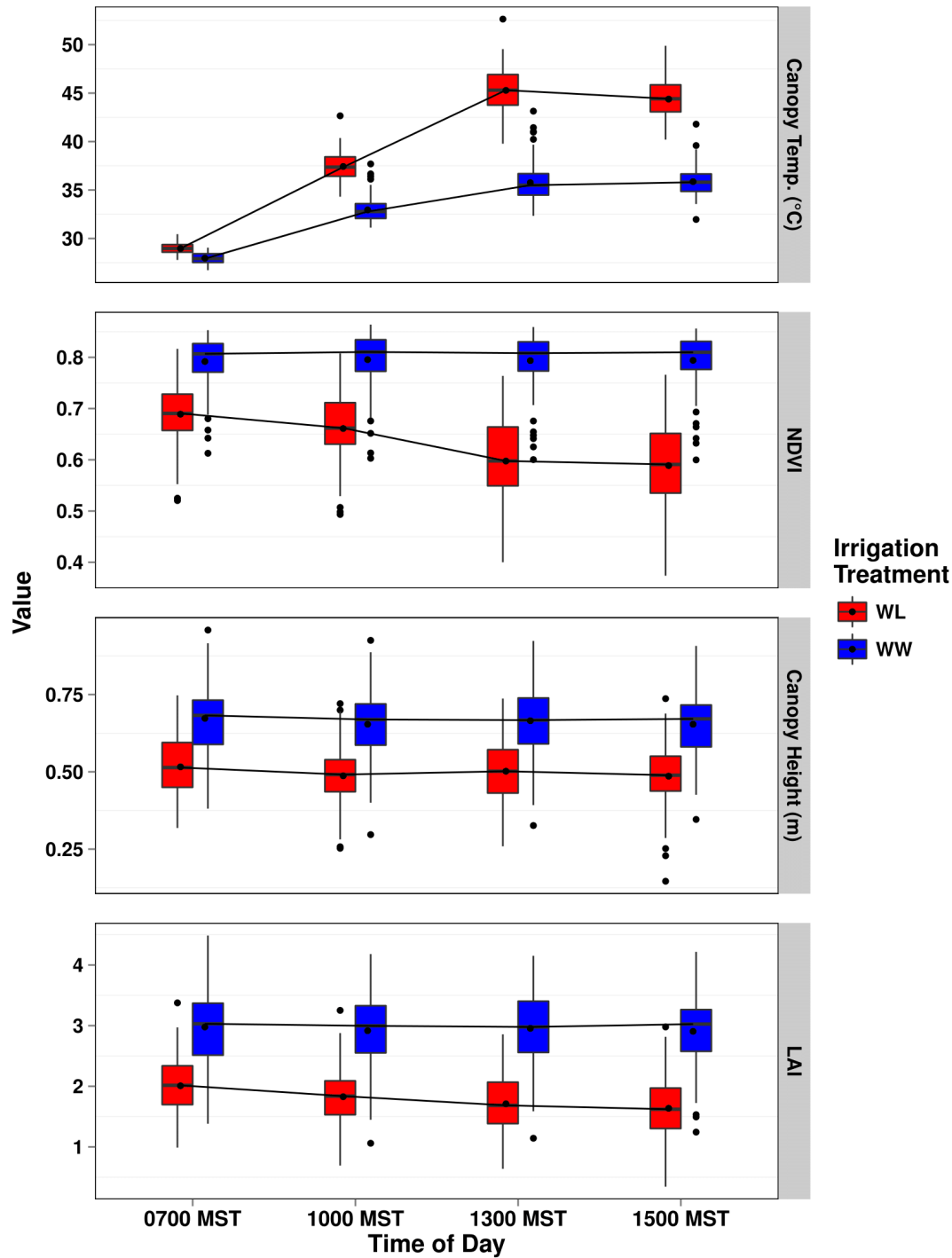
Figure 1. Comparison of best linear unbiased estimators (BLUEs) for canopy temperature (CT, degrees Celsius, top panel), normalized difference vegetation index (NDVI, unitless, second from top), canopy height (meters, third from top) and leaf area index (LAI, unitless, bottom panel) for the two irrigation regimes, water-limited (WL) and well-watered (WW), at four time points (0700, 1000, 1300, and 1500 MST) on day 222 (Julian calendar) in 2012.
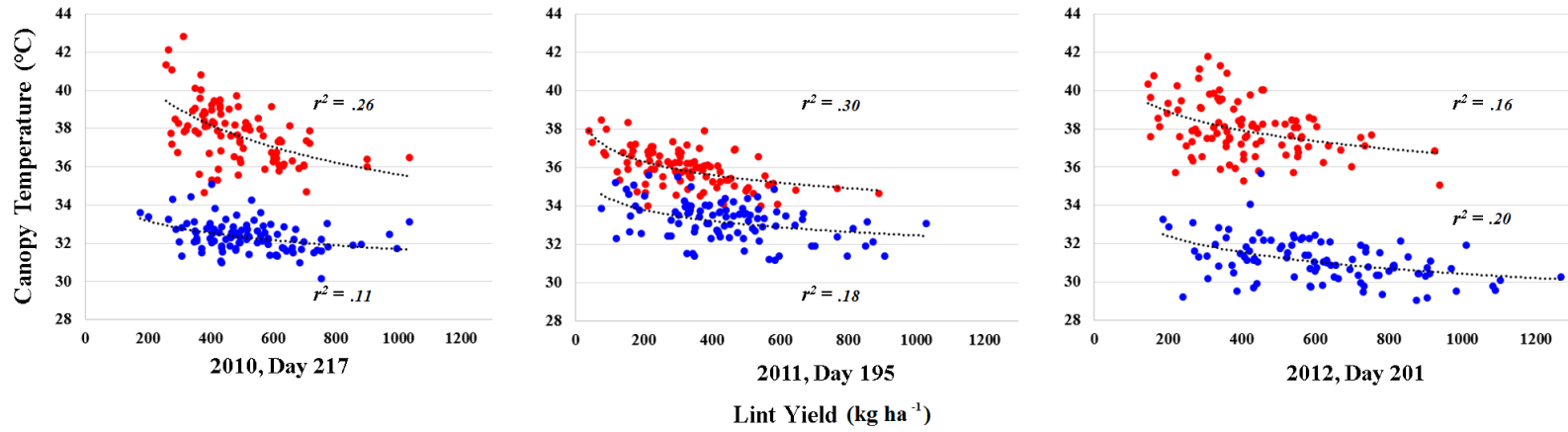
Figure 2. The degree of relationship (multiple r^2 from second order polynomial) between best linear unbiased estimators (BLUEs) of canopy temperature (°C) and lint yield (kg ha^{-1}) for the TM-1×NM24016 recombinant inbred line (RIL) population and its two parent lines evaluated under two irrigation regimes, water-limited (red) and well-watered (blue). The canopy temperature data were collected from three representative days during flowering/peak bloom within a year (Julian calendar) corresponding to 1300, 1500, 1300 MST for 2010, 2011, and 2012, respectively.
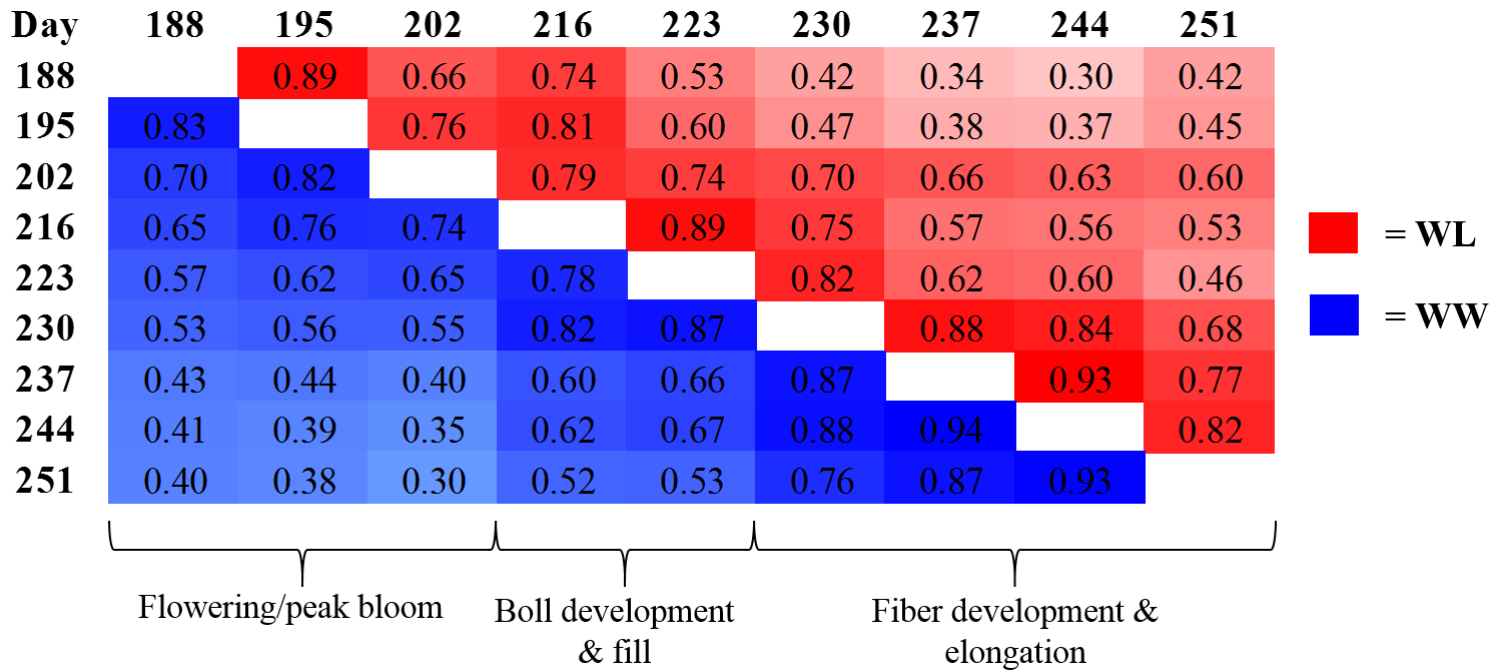
Day	188	195	202	216	223	230	237	244	251
188		0.89	0.66	0.74	0.53	0.42	0.34	0.30	0.42
195	0.83		0.76	0.81	0.60	0.47	0.38	0.37	0.45
202	0.70	0.82		0.79	0.74	0.70	0.66	0.63	0.60
216	0.65	0.76	0.74		0.89	0.75	0.57	0.56	0.53
223	0.57	0.62	0.65	0.78		0.82	0.62	0.60	0.46
230	0.53	0.56	0.55	0.82	0.87		0.88	0.84	0.68
237	0.43	0.44	0.40	0.60	0.66	0.87		0.93	0.77
244	0.41	0.39	0.35	0.62	0.67	0.88	0.94		0.82
251	0.40	0.38	0.30	0.52	0.53	0.76	0.87	0.93	

■ = WL
■ = WW

Flowering/peak bloom   Boll development & fill   Fiber development & elongation

Figure 3. Pearson correlation coefficients (r) for best linear unbiased estimators (BLUEs) of canopy temperature, calculated over all time points within a day, under two irrigation regimes, water-limited (red) and well-watered (blue), and their relationship to cotton developmental stages at different days (Julian calendar) throughout the 2011 growing season. All correlations were significant at $\alpha = 0.05$.
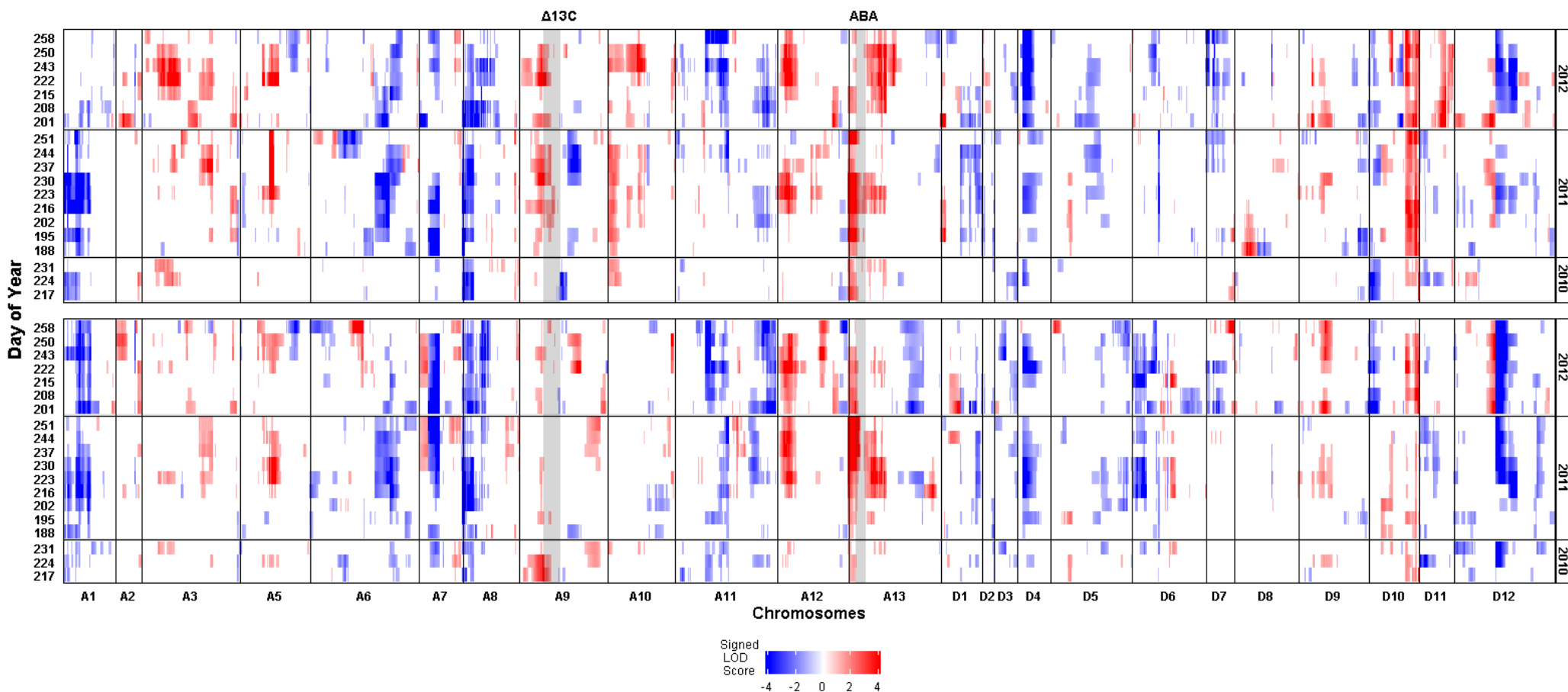
Figure 4. Genome-wide scan for quantitative trait loci (QTL) associated with canopy temperature across three years under two irrigation regimes, water-limited (WL, top panel) and well-watered (WW, bottom panel). Color is representative of the estimated additive allelic effect, with red and blue colors indicating increased and decreased canopy temperature, respectively, when substituting a NM24016 allele with an allele from TM-1. The intensity of the color represents the magnitude of the logarithm of odds (LOD) score with 3.3 as the significance threshold to declare QTL – values above 3.3 were assigned a value of 4 for presentation purposes. Shaded regions represent genomic intervals in which QTL were identified for carbon isotope discrimination and abscisic acid concentration (respective labels above graph). The left-hand y-axis denotes day of the growing season (Julian calendar) that data were collected, and the right-hand y-axis denotes year. The x-axis represents the mapped chromosomes of tetraploid cotton with marker intervals in centimorgans (cM). Chromosomes A04 and D13 did not have any mapped markers.

49